Thermodynamic and Kinetic Relationships between Lewis Acid−Lewis Base Complexes Relevant to the $P_2Pt(OTf)_2$-Catalyzed Diels−Alder Reaction

Nicole M. Brunkan, Peter S. White, and Michel R. Gagné*

Department of Chemistry, University of North Carolina at Chapel Hill, Chapel Hill, North Carolina 27599-3290

Received November 14, 2001

The Pt(II) Lewis acids $P_2Pt(OTf)_2$ (**2**; P_2 = dppe (**a**), *R*-BINAP (**b**)), which catalyze the Diels−Alder reaction of acryloyl-*N*-oxazolidinone (**4**) with cyclopentadiene (HCp), were generated in situ by activation of P_2Pt(*S*-BINOL) precursors **1** with 2 equiv of triflic acid (HOTf). Catalysts **2** and catalytically relevant Lewis acid−Lewis base complexes $[P_2Pt(L_2)]^{2+}$-$[OTf]^-_2$ (L_2 = 2 H_2O (**3**), dienophile **4** (**6**), Diels−Alder adduct **5** (**8**)) were characterized by ^1H and ^{31}P NMR spectroscopy at 195 K. **2a** was also characterized by X-ray crystallography. The thermodynamic relationships between **2**, **3**, **6**, **8**, and a BF_4^- analogue of **2** were determined through competitive binding experiments monitored by ^{31}P NMR at 195 K, to assess the effects of competitive inhibition of counterions, additives, and product on substrate coordination to the catalyst. These experiments demonstrated that the Lewis bases bind to $[P_2Pt]^{2+}$ with relative strengths $BF_4^- \ll OTf^- < \mathbf{4} < \mathbf{5} \ll H_2O$. The rates of two ligand exchange processes (dienophile/dienophile (k_1) and dienophile/OTf^- (k_2)) were measured at 270 K by simulation of exchange-broadened ^{31}P NMR spectra of **2**/**6** equilibrium mixtures, revealing that ligand substitution occurs more rapidly in the dppe system than the *R*-BINAP system (180 times faster for k_2). Finally, the reaction of HCp with **6** to give **8** was monitored by ^{31}P and ^1H NMR at 195 K; attack of HCp on Pt-coordinated **4** occurred much faster than ligand exchange, indicating that ligand exchange is the turnover-limiting step of the catalytic cycle.

Introduction

Stereoselective carbon−carbon bond-forming reactions catalyzed by chiral, electrophilic transition-metal Lewis acid complexes have become essential tools for the synthesis of many enantiopure organic molecules.[1] Although Lewis acids containing transition metals from nearly all regions of the periodic table, from Sc(III) to Zn(II),[1b] have been utilized as catalysts for these transformations, more attention has historically been devoted to the study of early-metal and Cu(II)/Zn(II)[2] catalysts than to examination of Lewis acids based on group 8−10 metals. For example, the chemistry of well-defined, chiral Ru(II)- and Fe(II)-based Lewis acids (group 8) has only recently been developed,[3] while group 9 Lewis acid catalysts are even more rare.[4] From group 10, chiral octahedral Ni(II) coordination compounds have been used as enantioselective Lewis acid catalysts by Kanemasa.[5] However, the most numerous catalysts from this "center-right" area of the periodic table are the dicationic, square-planar, diphosphine-based Pd(II) and Pt(II) Lewis acids that have emerged over the last several years.[6] Because their stereoelectronic properties are inherently different from those of early transition metals and the first-row late metals Cu(II) and Zn(II), these $[P_2M]^{2+}[A]^-_2$ (P_2 = diphosphine; M = Pd or Pt; A^- = OTf^-, BF_4^-, PF_6^-, SbF_6^-, ClO_4^-) Lewis acids have

(1) (a) Jacobsen, E. N.; Pfaltz, A.; Yamamoto, H., Eds. *Comprehensive Asymmetric Catalysis*; Springer-Verlag: Berlin, 1999; pp 912−1306. (b) Yamamoto, H., Ed. *Lewis Acids in Organic Synthesis*; Wiley-VCH: New York, 2000. (c) Noyori, R. *Asymmetric Catalysis in Organic Synthesis*; Wiley: New York, 1994. (d) Carmona, D.; Lamata, M. P.; Oro, L. A. *Coord. Chem. Rev.* **2000**, *200−202*, 717−772. (e) Jørgensen, K. A. *Angew. Chem., Int. Ed.* **2000**, *39*, 3558−3588. (f) Dias, L. C. *J. Braz. Chem. Soc.* **1997**, *8*, 289−332.

(2) Cu: (a) Johnson, J. S.; Evans, D. A. *Acc. Chem. Res.* **2000**, *33*, 325−335. (b) Jørgensen, K. A.; Johanssen, M.; Yao, S.; Audrain, H.; Thorhauge, J. *Acc. Chem. Res.* **1999**, *32*, 605−613.

(3) Fe: (a) Kündig, E. P.; Bourdin, B.; Bernardinelli, G. *Angew. Chem., Int. Ed. Engl.* **1994**, *33*, 2856−1857. (b) Bruin, M. E.; Kündig, E. P. *Chem. Commun.* **1998**, 2635−2636. Ru: (c) Kündig, E. P.; Saudan, C. M.; Bernardinelli, G. *Angew. Chem., Int. Ed.* **1999**, *38*, 1219−1223. (d) Carmona, D.; Cativiela, C.; Elipe, S.; Lahoz, F. J.; Lamata, M. P.; López-Ram de Víu, M. P.; Oro, L. A.; Vaga, C.; Viguri, F. *Chem. Commun.* **1997**, 2351−2352. (e) Davenport, A. J.; Davies, D. L.; Fawcett, J.; Garratt, S. A.; Russell, D. R. *J. Chem. Soc., Dalton Trans.* **2000**, 4432−4441. (f) Faller, J. W.; Grimmond, B. J. *Organometallics* **2001**, *20*, 2454−2458.

(4) (a) Davenport, A. J.; Davies, D. L.; Fawcett, J.; Garratt, S. A.; Lad, L.; Russell, D. R. *Chem. Commun.* **1997**, 2347−2348. (b) Carmona, D.; Lahoz, F. J.; Elipe, S.; Oro, L. A.; Lamata, M. P.; Viguri, F.; Mir, C.; Cativiela, C.; Viu, M. P. L.-R. d. *Organometallics* **1998**, *17*, 2986−2995.

(5) (a) Kanemasa, S.; Kanai, T. *J. Am. Chem. Soc.* **2000**, *122*, 10710−10711. (b) Kanemasa, S.; Oderaotoshi, Y.; Sakaguchi, S.; Yamamoto, H.; Tanaka, J.; Wada, E.; Curran, D. P. *J. Am. Chem. Soc.* **1998**, *120*, 3074−3088.

(6) (a) Ghosh, A. K.; Matsuda, H. *Org. Lett.* **1999**, *1*, 2157−2159. (b) Pignat, K.; Vallotto, J.; Pinna, F.; Strukul, G. *Organometallics* **2000**, *19*, 5160−5167. (c) Hao, J.; Hatano, M.; Mikami, K. *Org. Lett.* **2000**, *2*, 4059−4062. (d) Oi, S.; Terada, E.; Ohuchi, K.; Kato, T.; Tachibana, Y.; Inoue, Y. *J. Org. Chem.* **1999**, *64*, 8660−8667, and ref 12 and 13 therein. (e) Hattori, T.; Suzuki, Y.; Uesugi, O.; Oi, S.; Miyana, S. *Chem. Commun.* **2000**, 73−74. (f) Ferraris, D.; Young, B.; Dudding, T.; Lectka, T. *J. Am. Chem. Soc.* **1998**, *120*, 4548−4549. (g) Hori, K.; Kodama, H.; Ohta, T.; Furukawa, I. *J. Org. Chem.* **1999**, *64*, 5017−5023. (h) Hori, K.; Ito, J.; Ohta, T.; Furukawa, I. *Tetrahedron* **1998**, *54*, 12737−12744. (i) Fürstner, A.; Voigtländer, D.; Schrader, W.; Giebel, D.; Reetz, M. T. *Org. Lett.* **2001**, *3*, 417−420.

10.1021/om0109861 CCC: $22.00
Publication on Web 03/19/2002

the potential to uniquely affect the reactivity and selectivity of the reactions they catalyze.

One significant difference between $[P_2M]^{2+}$ Lewis acids and their early metal or first-row counterparts is the softness of the Pd and Pt metal centers, which increases their carbophilicity relative to their oxophilicity.[7] The effects of this enhanced carbophilicity on the coordination chemistry of P_2M^{II} complexes include preferential binding of enolate ligands via metal−carbon rather than metal−oxygen bonds.[8] The observation of unorthodox C,O binding modes for binaphthol or biphenanthrol-type ligands in sterically congested Pt and Pd complexes (in contrast to the O,O′-binding modes seen in early-transition-metal compounds) has also been attributed to the greater softness of the group 10 metals.[9] With respect to catalysis, the impact of the carbophilicity of a $[P_2Pd]^{2+}[A]^{-}_2$ Lewis acid catalyst on the mechanism of imine and aldehyde alkylation by Mukaiyama-type nucleophiles was demonstrated recently in work by Sodeoka and by Fujimura.[10] In polar solvents at relatively high reaction temperatures, these reactions were found to proceed through C-bound Pd enolate intermediates formed by reaction of the catalyst with the nucleophile, rather than by traditional Lewis acid activation of the aldehyde or imine substrates via Pd−O or Pd−N coordination. This behavior is unprecedented with conventional early metal Lewis acid catalysts. However, the same $[P_2Pd]^{2+}[A]^{-}_2$ catalyst may also act as a traditional Lewis acid in analogous reactions involving more activated imine substrates, lower reaction temperatures, and less polar solvents, as demonstrated by Lectka.[6f]

The lability of ligands coordinated to the metal center may also differ greatly in complexes involving early- and late-transition-metal Lewis acids. Square-planar, 16-electron Pd(II) and especially Pt(II) complexes undergo ligand exchange reactions much more slowly than complexes containing substitutionally labile, octahedral early-metal centers or first-row metals such as Cu(II) or Zn(II).[1b] Moreover, ligand exchange almost always proceeds via associative mechanisms in P_2M^{II} complexes,[11] even when extremely weakly coordinated ligands such as σ-bound methane are involved.[12] Since substrate/product ligand exchange is essential to achieve turnover in a Lewis acid catalyzed reaction, the unique ligand exchange characteristics peculiar to group 10 complexes may be important in defining the mechanisms of $[P_2M]^{2+}$-catalyzed reactions.

Scheme 1

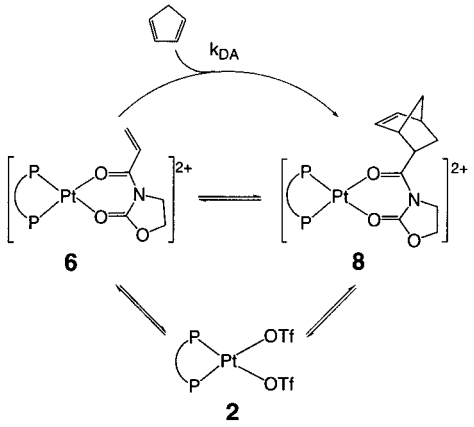

Clearly, group 10 $[P_2M]^{2+}$ transition-metal complexes have the potential to exhibit new and beneficial reactivity, compared to traditional p-block, early-metal, and Cu(II)/Zn(II) Lewis acids, when employed as catalysts for organic transformations. Thus far, however, the mechanisms of $[P_2M]^{2+}$-catalyzed reactions have not been investigated in sufficient detail to understand or predict the diverse reactivity offered by these Pd and Pt Lewis acids. Therefore, we have undertaken a comprehensive investigation of the Pt(II) Lewis acids $P_2Pt(OTf)_2$ (**2**; P_2 = dppe (**a**), *R*-BINAP (**b**)) and their

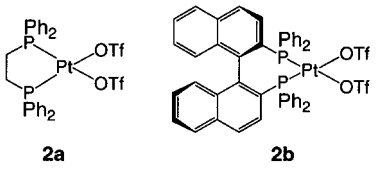

activity as catalysts for the Diels−Alder reaction of acryloyl-*N*-oxazolidinone (**4**) with cyclopentadiene (HCp; eq 1), with the ultimate aim of understanding the

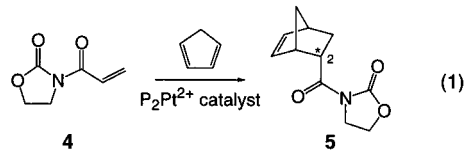

fundamental principles underlying the mechanism(s) available to these catalysts. Specific questions addressed during the research include the following. (1) Do the reactions proceed via a true Lewis acid mechanism: i.e., does the catalyst activate the substrate by coordination of the dienophile to Pt through the carbonyl groups (Scheme 1)? (2) Does competitive coordination of counterions, product, or additives inhibit substrate binding to the catalyst? (3) What is the turnover-limiting step of the catalytic cycle? (4) How do the stereoelectronic properties of the diphosphine ligand P_2 affect the behavior of the Lewis acid catalyst?

Note that questions such as the first three above are of general interest for many Lewis acid catalyzed reactions; however, the data needed to answer them are difficult to obtain for most p-block, early-transition-

(7) Pearson, R. G. *Hard and Soft Acids and Bases*; Dowden, Hutchinson, and Ross: Stroudsburg, PA, 1973.

(8) (a) Veya, P.; Floriani, C.; Chiesi-Villa, A.; Risoli, C. *Organometallics* **1993**, *12*, 4899−4907. Examples of late-metal C-bound enolates: (b) Bergman, R. G.; Kaplan, A. W. *Organometallics* **1997**, *16*, 1106−1108. (c) Hsu, R. H.; Chen, J. T.; Lee, G. H.; Wang, Y. *Organometallics* **1997**, *16*, 1159−1166. (d) Hamann, B. C.; Hartwig, J. F. *J. Am. Chem. Soc.* **1997**, *119*, 12382−12383. A late-metal O-bound enolate: (e) Slough, G. A.; Bergman, R. G.; Heathcock, C. H. *J. Am. Chem. Soc.* **1989**, *111*, 938−949.

(9) (a) Brunkan, N. M.; White, P. S.; Gagné, M. R. *J. Am. Chem. Soc.* **1998**, *120*, 11002−11003. (b) Bergens, S. H.; Leung, P.-H.; Bosnich, B. *Organometallics* **1990**, *9*, 2406−2408. (c) See also: Kocovsky, P.; Vyskocil, S.; Cisarova, I.; Sejbal, J.; Tislerova, I.; Smrcina, M.; Lloyd-Jones, G. C.; Stephen, S. C.; Butts, C. P.; Murray, M.; Langer, V. *J. Am. Chem. Soc.* **1999**, *121*, 7714−7715.

(10) (a) Fujii, A.; Hagiwara, E.; Sodeoka, M. *J. Am. Chem. Soc.* **1999**, *121*, 5450−5458. (b) Fujii, A.; Sodeoka, M. *Tetrahedron Lett.* **1999**, *40*, 8011−8014. (c) Fujimura, O. *J. Am. Chem. Soc.* **1998**, *120*, 10032−10039.

(11) Cross, R. J. *Adv. Inorg. Chem.* **1989**, *34*, 219−292.

(12) Johansson, L.; Tilset, M. *J. Am. Chem. Soc.* **2001**, *123*, 739−740.

metal, or even Cu(II)/Zn(II) Lewis acids.[13] For example, solid-state[14] or in situ characterization[15] of only a few catalyst–substrate or catalyst–product complexes has been reported, while issues such as competitive coordination of counterions, reaction products, or additives to the catalyst have rarely been addressed.[15a] The $P_2Pt(OTf)_2$ Lewis acids examined here, on the other hand, are uniquely suited to mechanistic studies because of their good stability, convenient catalytic rates, and slow rates of ligand substitution reactions and because of the fact that they contain spin-active ^{31}P and ^{195}Pt nuclei. These characteristics enabled direct, in situ observation of active catalysts, catalyst–substrate and catalyst–product complexes using ^{31}P and ^{1}H NMR spectroscopy, made investigation of both the thermodynamic relationships between the complexes and the kinetics of ligand exchange reactions feasible via ^{31}P NMR experiments, and even facilitated direct observation of Pt-catalyzed Diels–Alder reactions at low temperature by ^{31}P and ^{1}H NMR.

The results of our examination of $P_2Pt(OTf)_2$ Lewis acid Diels–Alder catalysts are presented in two consecutive papers. This paper describes a detailed investigation of the binding of catalytically relevant Lewis bases (counterions, substrate, product, and water) to the $[P_2Pt]^{2+}$ Lewis acid catalysts. The Lewis acids **2** were generated in situ, characterized spectroscopically and crystallographically (P_2 = dppe), and allowed to react with Lewis bases, forming complexes that were characterized by ^{31}P and ^{1}H NMR at 195 K. The relative binding strengths of the Lewis bases to $[P_2Pt]^{2+}$ were determined through competition experiments, the kinetics of ligand exchange were explored via simulation of dynamic ^{31}P NMR spectra, and the relative rates of ligand exchange vs cycloaddition were revealed when **2**-catalyzed Diels–Alder reactions (eq 1) were monitored by NMR at 195 K. The second paper (immediately following) describes the last experiments more thoroughly, since they revealed that the Pt Lewis acids undergo an unusual decomposition reaction under catalysis conditions and that phosphine-dependent decomposition rates actually cause the Diels–Alder reaction to proceed via different mechanisms when P_2 = dppe vs *R*-BINAP.[16] Note that the *R*-BINAP catalyst **2b** was examined initially because Ghosh reported that 20 mol % of it, prepared by protonation of [*R*-BINAP]-Pt(salicylate) with 2 equiv of triflic acid (HOTf), catalyzed the Diels–Alder reaction (eq 1) in 96–98% ee.[6a] Ghosh also found that addition of 2 equiv of water to the reaction mixture dramatically increased the turnover rate (complete conversion in 1 h rather than 20 h at −40 °C).[6a] The dppe Lewis acid **2a** was of interest because it is a soluble model for a Lewis acid in a molecularly imprinted polymer,[17] which we hoped to generate by protonation of a polymer-imprinted analogue of **1a** with 2 equiv of HOTf (Scheme 2, vide infra), as part of our ongoing research into the effect of associated chiral cavities on molecularly imprinted catalysts.[18]

Scheme 2

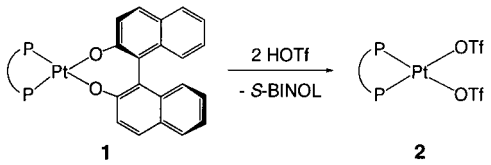

1 **2**

Results

(1) Formation and Characterization of $P_2Pt(OTf)_2$ (2). The Pt(II) Lewis acids $P_2Pt(OTf)_2$ (**2**; P_2 = dppe (**a**); *R*-BINAP (**b**)) were generated in situ from the yellow air- and water-stable precursors P_2Pt(*S*-BINOL) (**1**), which were prepared as previously described.[19] Protonation of **1** with 2 equiv of freshly distilled triflic acid (HOTf) at room temperature in CD_2Cl_2 under dry conditions cleanly generated new, colorless, symmetric P_2Pt species that were assigned to **2** on the basis of ^{1}H and ^{31}P NMR data (Scheme 2; Table 1).[20] The 530–540 Hz increase in the P–Pt coupling constant on conversion of **1** to **2** was diagnostic, as it indicated that BINOL was replaced by a ligand (triflate) that exerts a poorer trans influence on phosphorus and is therefore more weakly coordinated to Pt than BINOL.[21] One equivalent of free *S*-BINOL was observed by ^{1}H NMR.

When the **1a** protonation reaction was carried out in dry chlorobenzene rather than CD_2Cl_2, colorless single crystals of **2a** were obtained from the solution upon standing overnight. X-ray crystallographic analysis yielded the structure shown in Figure 1. Rigorously dry conditions were necessary to isolate **2a**, since the bis(aqua) complex $[(dppe)Pt(OH_2)_2]^{2+}[OTf]^{-}_2$ (**3a**) is also crystalline and very stable (Scheme 3).[22] Only one other $P_2Pt(OTf)_2$ species, $[1,2\text{-}C_6H_4(PMePh)_2]Pt(OTf)_2$, has

(13) Notable exceptions: (a) Jacquith, J. B.; Levy, C. J.; Bondar, G. V.; Wang, S.; Collins, S. *Organometallics* **1998**, *17*, 914–925. (b) Lin, S.; Bondar, G. V.; Levy, C. J.; Collins, S. *J. Org. Chem.* **1998**, *63*, 1885–1892. (c) Bonnesen, P. V.; Puckett, C. L.; Honeychuck, R. V.; Hersh, W. H. *J. Am. Chem. Soc.* **1989**, *111*, 6070–6081.

(14) Crystallographic characterization of catalyst–substrate complexes: (a) Shambayati, S.; Crowe, W. E.; Schreiber, S. L. *Angew. Chem., Int. Ed. Engl.* **1990**, *29*, 256–272. (b) Gothelf, K.; Hazell, R. G.; Jørgensen, K. A. *J. Am. Chem. Soc.* **1995**, *117*, 4435–4436. (c) Evans, D. A.; Rovis, T.; Kozlowski, M. C.; Downey, W.; Tedrow, J. S. *J. Am. Chem. Soc.* **2000**, *122*, 9134–9142. See also ref 3d,e.

(15) In situ investigation (by ^{1}H NMR) of the interactions of substrates with p-block catalysts such as BF_3, $SnCl_4$, and $MeAlCl_2$: (a) Hunt, I. R.; Rogers, C.; Woo, S.; Rauk, A.; Keay, B. R. *J. Am. Chem. Soc.* **1995**, *117*, 1049–1056. (b) Denmark, S. E.; Almstead, N. G. *J. Am. Chem. Soc.* **1993**, *115*, 3133–3139. (c) Denmark, S. E.; Henke, B. R.; Weber, E. *J. Am. Chem. Soc.* **1987**, *109*, 2512–2514. (d) Castellino, S. *J. Org. Chem.* **1990**, *55*, 5197–5200. (e) Castellino, S.; Dwight, W. J. *J. Am. Chem. Soc.* **1993**, *115*, 2986–2987. (f) Childs, R. F.; Mulholland, D. L.; Nixon, A. *Can. J. Chem.* **1982**, *60*, 801–808. (g) Hawkins, J. M.; Loren, S.; Nambu, M. *J. Am. Chem. Soc.* **1994**, *116*, 1657–1660. (h) Gajewski, J. J.; Ngernmeesri, P. *Org. Lett.* **2000**, *2*, 2813–2815. (i) Corey, E. J.; Loh, T.-P.; Sarshar, S.; Azimioara, M. *Tetrahedron Lett.* **1992**, *33*, 6945–6948. (j) Cardillo, G.; Gentilucci, L.; Gianotti, M.; Tolomelli, A. *Org. Lett.* **2001**, *3*, 1165–1167.

(16) See: Brunkan, N. M.; Gagné, M. R. *Organometallics* **2002**, *21*, 1576–1582.

(17) For reviews of molecular imprinting see: (a) *Molecularly Imprinted Polymers: Man-made Mimics of Anitbodies and Their Applications in Analytical Chemistry;* Sellergren, B., Ed.; Elsevier: Amsterdam, 2001. (b) Wulff, G. *Angew. Chem., Int. Ed. Engl.* **1995**, *34*, 1812–1832.

(18) Brunkan, N. M.; Gagné, M. R. *J. Am. Chem. Soc.* **2000**, *122*, 6217–6225.

(19) Brunkan, N. M.; White, P. S.; Gagné, M. R. *Angew. Chem., Int. Ed.* **1998**, *37*, 1579–1582.

(20) See the Supporting Information for the ^{1}H NMR spectrum.

(21) (a) Pidcock, A.; Richards, R. E.; Venanzi, L. M. *J. Chem. Soc. A* **1966**, 1701–1710. (b) Appleton, T. G.; Bennett, M. A. *Inorg. Chem.* **1978**, *17*, 738–747.

(22) (a) Fallis, S.; Anderson, G. K.; Rath, N. P. *Organometallics* **1991**, *10*, 3180–3184. (b) Gorla, F.; Venanzi, L. M. *Helv. Chim. Acta* **1990**, *73*, 690–697.

Table 1. ^{31}P NMR Data for P_2Pt^{II} Complexes in CD_2Cl_2

Pt complex	temp (K)	δ (ppm)	$^1J_{P-Pt}$[a] (Hz)	$^2J_{P-P}$ (Hz)
(dppe)Pt(*S*-BINOL) (**1a**)	room temp	27.2	3640	
(*R*-BINAP)Pt(*S*-BINOL) (**1b**)	room temp	5.2	3670	
(dppe)Pt$(OTf)_2$ (**2a**)	195	40.4	4170	
(*R*-BINAP)Pt$(OTf)_2$ (**2b**)	195	1.6	4210	
[(dppe)Pt$(OH_2)_2]^{2+}[OTf^-]_2$ (**3a**)	195	37.7	3950	
[(***R***-BINAP)Pt$(OH_2)_2]^{2+}[OTf^-]_2$ (**3b**)	195	3.5	4050	
[(dppe)Pt(**4**)$]^{2+}[OTf^-]_2$ (**6a**)	195	39.9	4080	9.7
		35.9	4000	
[(*R*-BINAP)Pt(**4**)$]^{2+}[OTf^-]_2$ (**6b**)	195	3.8	4200	27.4
		2.9	3990	
[(dppe)Pt(**4**)$]^{2+}[BF_4^-]_2$ (**7a**)	195	39.9	4080	9.7
		36.0	3990	
[(*R*-BINAP)Pt(**4**)$]^{2+}[BF_4^-]_2$ (**7b**)	195	4.0	4270	27.4
		2.6	4050	
[(dppe)Pt(*2S*-**5**)$]^{2+}[OTf^-]_2$ (**8a**)	195	39.5	4110	10.6
		36.4	4020	
[(*R*-BINAP)Pt(*2S*-**5**)$]^{2+}[OTf^-]_2$ (*R*,*2S*-**8b**)	195	3.6	4210	27.5
		2.8	4020	
[(*R*-BINAP)Pt(*2R*-**5**)$]^{2+}[OTf^-]_2$ (*R*,*2R*-**8b**)	195	3.3	4210	27.7
		3.0	4020	

[a] $^1J_{P-Pt}$ values determined from spectra acquired at 195 K have ±30 Hz uncertainty, as Pt satellites were very broad at this temperature.

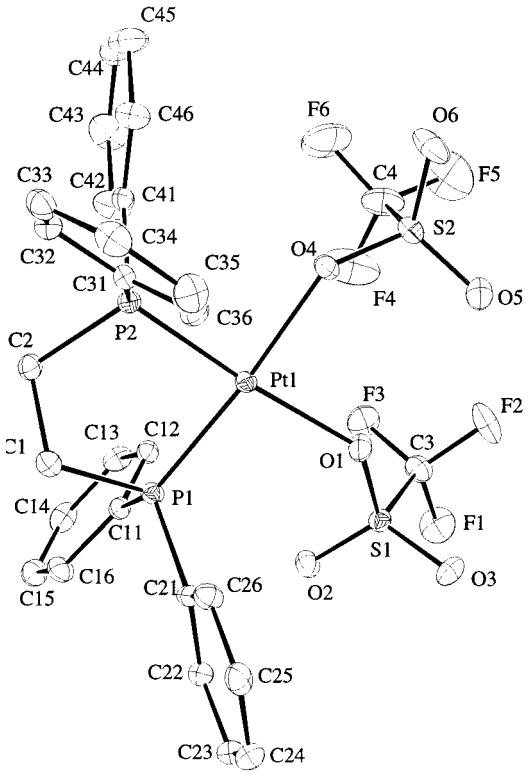

Figure 1. ORTEP drawing of (dppe)Pt$(OTf)_2$ (**2a**). Selected bond lengths (Å): Pt−P_1 = 2.2158(14), Pt−P_2 = 2.2151(14), Pt−O_1 = 2.120(4), Pt−O_2 = 2.138(4). Selected bond angles (deg): P_1−Pt−P_2 = 85.74(5), O_1−Pt−O_4 = 87.51(15), P_1−Pt−O_1 = 98.69(11), P_2−Pt−O_4 = 87.98(11).

been crystallographically characterized;[23] bond lengths and angles for **2a** (Figure 1) are similar (within 0.01 Å and 7°, respectively) to those of the 1,2-C_6H_4(PMePh)$_2$ complex. Although a few crystals of **2a** were isolated for X-ray analysis, attempts to prepare macroscopic quantities of **2** were unsuccessful, as the isolated products always contained the diaqua complex **3**. Thus, **2** was prepared in situ from **1** and used immediately.

(23) Appelt, A.; Ariaratnam, V.; Willis, A. C.; Wild, S. B. *Tetrahedron: Asymmetry* **1990**, *1*, 9−12. Also note that the $^1J_{P-Pt}$ value for [1,2-C_6H_4(PMePh)$_2$]Pt$(OTf)_2$ is 4034 Hz, 140 Hz smaller than that of **2a**.

Scheme 3

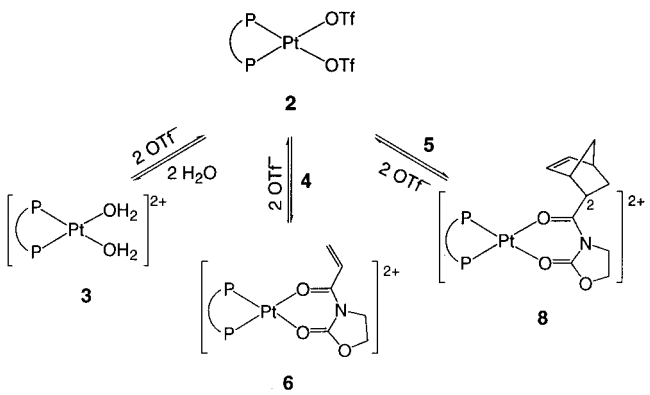

(2) Formation and Characterization of $[P_2Pt(L_2)]^{2+}[OTf]^-_2$. Addition of neutral, Lewis basic ligands L_2 (L_2 = 2 H_2O, acryloyl-*N*-oxazolidinone (**4**), Diels−Alder adduct (**5**)) to $P_2Pt(OTf)_2$ in CD_2Cl_2 solution at room temperature generated the Lewis acid−Lewis base adducts $[P_2Pt(L_2)]^{2+}[OTf]^-_2$ (Scheme 3), which were characterized by ^{31}P and ^{1}H NMR at 195 K (Table 1).[20] In the case of water, adding 2 equiv quantitatively converted **2** to **3**; however, addition of up to 10 equiv of **4** or **5** to **2** produced an equilibrium mixture of **2** and the Lewis acid−Lewis base complex **6** or **8**. At 195 K, OTf^-/L_2 exchange was slow on the NMR time scale, and separate sharp resonances for the $[P_2Pt(L_2)]^{2+}[OTf]^-_2$ and residual $P_2Pt(OTf)_2$ species were observed; at room temperature, rapid OTf^-/L_2 exchange produced a single broad resonance in the ^{31}P NMR spectra of some of the reaction mixtures (vide infra).

The P−Pt coupling constant of the symmetric diaqua complex **3** was found to be ∼200 Hz smaller than that of **2**, indicating that water coordinates more strongly to Pt than does triflate (Table 1).[21] In the case of **3a,** the Pt-coordinated water resonates at 7.28 ppm in the ^{1}H NMR spectrum.[20] The white air- and water-stable dppe complex **3a** was isolated as described in the literature;[22] however, analogous attempts to isolate **3b** cleanly yielded the μ-OH dimer $[(R\text{-BINAP})Pt(\mu\text{-OH})]_2^{2+}$-$[OTf]^-_2$ instead of the desired diaqua species.[24,25]

Pt−oxazolidinone complexes **6** were generated by adding 2 equiv of HOTf to **1** (forming **2** in situ) in the

Scheme 4

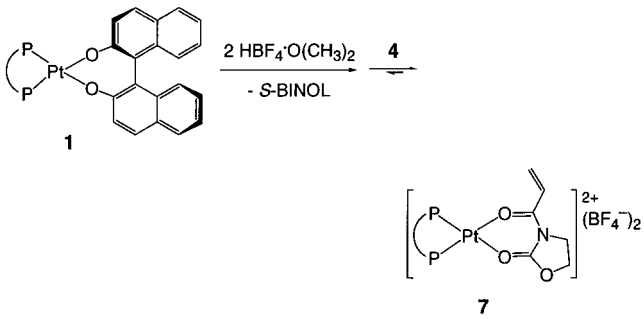

presence of 2–10 equiv of dienophile **4**. ^{31}P NMR spectra of **6** consisted of two doublets with Pt satellites, with P–Pt coupling constants slightly smaller (10–220 Hz) than those of the corresponding $P_2Pt(OTf)_2$ species (Table 1). The loss of symmetry in **6** and the magnitudes of the P–Pt coupling constants are consistent with the expected (and productive) bidentate coordination of **4** to Pt through its carbonyl oxygens (Scheme 3). Resonances for coordinated **4** were also well-separated from free **4** in the ^1H NMR spectrum.[20] Similar Pt–oxazolidinone complexes with BF_4^- rather than OTf^- counterions were obtained by protonation of **1** with 2 equiv of $HBF_4{\cdot}OMe_2$ in the presence of 5 equiv of **4** (Scheme 4). Although protonation of **1** with $HBF_4{\cdot}OMe_2$ in the absence of **4** generates a mixture of symmetric and asymmetric species by ^{31}P NMR,[26] $[P_2Pt(\mathbf{4})]^{2+}[BF_4]^-_2$ (**7**) formed quantitatively when **4** was present, producing NMR spectra almost identical with those of **6** (Table 1).

Generating **2** in the presence of 1.5–2 equiv of enantioenriched Diels–Alder adduct 2*S*-**5** (95% endo, 92% ee) yielded Pt-*endo*-**5** complexes $[P_2Pt(2S\text{-}\mathbf{5})]^{2+}$-$[OTf]^-_2$ (**8a** and *R*,2*S*-**8b**), with ^{31}P NMR spectra similar to those of the Pt–oxazolidinone complexes **6**, as the major reaction products (~90%; Scheme 3). Additionally, four to five minor asymmetric species that could not be identified were observed by ^{31}P NMR in the dppe reaction (see Figure 2), while a single minor species was present in the *R*-BINAP case. Using racemic rather than enantioenriched Diels–Alder adduct **5** (90% endo) for the *R*-BINAP reaction produced the same major species, which was now accompanied by a different minor species (35%). This new species was assigned to the diastereomer $[(R\text{-BINAP})Pt(2R\text{-}\mathbf{5})]^{2+}[OTf]^-_2$ (*R*,2*R*-**8b**), formed when the 2*R* rather than the 2*S* enantiomer of **5** coordinates to the chiral $[(R\text{-BINAP})Pt]^{2+}$ fragment.[27] Resonances for free **5**, coordinated 2*S*-**5**, and coordinated 2*R*-**5** were distinguishable in the ^1H NMR spectrum.[20] In catalytic reactions, (*R*-BINAP)$Pt(OTf)_2$ produces 2*S*-**5** as the major product (96–98% ee).[6a]

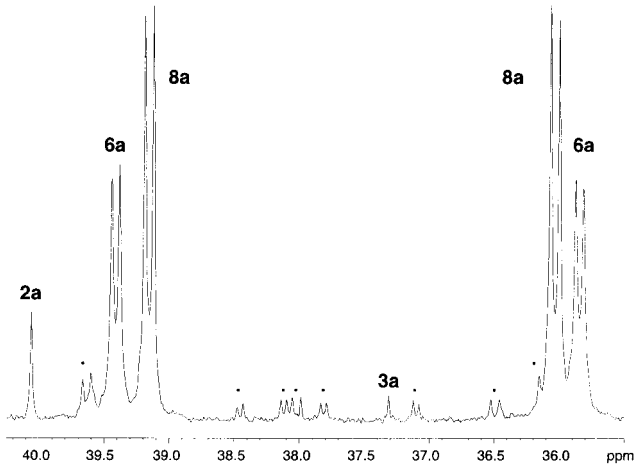

Figure 2. ^{31}P NMR spectrum (400 MHz) of an experiment in which **4** and 2*S*-**5** competed for coordination to **2a**, yielding an equilibrium mixture of **6a** and **8a** (entry 5, Table 2). **3a** is an impurity, and • denotes unidentified asymmetric minor products of the reaction of **2a** with 2*S*-**5**. Platinum satellites are not shown.

(3) Measurement of Equilibrium Constants for the Relative Binding of Lewis Bases to $[P_2Pt]^{2+}$. The relative abilities of the OTf^- and BF_4^- counterions and neutral ligands L_2 to coordinate to the $[P_2Pt]^{2+}$ Lewis acids were quantified by measuring equilibrium constants (K_{eq}) for the reactions in Table 2. The data in entries 1–3 were derived from the experiments described in section 2 as follows: K_{eq} values for the **2**/**6** (OTf^-/**4**) equilibria in entry 1 were calculated via integration of the ^{31}P NMR resonances for Pt–oxazolidinone complex **6** and residual **2** in spectra obtained when **2** was generated in the presence of 2–10 equiv of **4**. The data in entry 2 represent a lower limit of K_{eq} for the **2**/**3** (OTf^-/OH_2) equilibrium, since addition of only 2 equiv of water to **2** completely converted it to diaqua complex **3**. Similarly, entry 3 represents a lower limit of K_{eq} for the "$P_2Pt(BF_4)_2$"/**7** (BF_4^-/**4**) equilibrium, as addition of 5 equiv of **4** to the Lewis acid generated by protonation of **1** with $HBF_4{\cdot}OMe_2$ quantitatively produced **7**.

Thermodynamic relationships between the cationic complexes $[P_2Pt(L_2)]^{2+}[OTf]^-_2$ were explored through experiments in which two different ligands L_2 competed for binding to **2**. For example, the abilities of **4** and **5** to compete with water for coordination to Pt were tested by exposing isolated dppe diaqua complex **3a** to 10 equiv of either **4** or *rac*-**5** in CD_2Cl_2 solution. 195 K ^{31}P NMR spectra of these reactions showed no trace of **6a** or **8a**, allowing calculation of the upper limit of K_{eq} for the **3**/**6** (H_2O/**4**) and **3**/**8** (H_2O/**5**) equilibria in entry 4 (Table 2). In the *R*-BINAP case, nonisolable diaqua complex **3b** was generated in situ by titration of **2b** with a stock solution of water in CH_2Cl_2 until 98–99% pure **3b** was attained (by ^{31}P NMR), and then 10 equiv of **4** or **5** was added to the reaction mixture. Initially, 10 equiv of **4** appeared to convert 10% of **3b** to **6b**; however, adding 10 equiv more of **4** to the reaction did *not* increase the

(24) The complex $\{[R\text{-BINAP}]Pt(OH_2)_2]^{2+}$ (**3b**) has not been reported, although the Pd analogue and the monoaqua complex species $\{[R\text{-BINAP}]Pt(OH_2)(OTf)\}^+[OTf]^-$ are known: (a) Fujii, A.; Hagiwara, E.; Sodeoka, M. *J. Am. Chem. Soc.* **1999**, *121*, 5450–5458. (b) Fujii, A.; Sodeoka, M. *Tetrahedron Lett.* **1999**, *40*, 8011–8014. (c) Stang, P. J.; Olenyuk, B.; Arif, A. M. *Organometallics* **1995**, *14*, 5281–5289.

(25) Complexes of the type $[P_2Pt(\mu\text{-}OH)]_2^{2+}$ are well-known; see for example: (a) Bandini, A. L.; Banditelli, G.; Demartin, F.; Manassero, M.; Minghetti, G. *Gazz. Chim. Ital.* **1993**, *123*, 417–423. (b) Li, J. J.; Li, W.; Sharp, P. R. *Inorg. Chem.* **1996**, *35*, 604–613.

(26) The symmetric ($^1J_{P-Pt} \approx 4100$ Hz) and one of the asymmetric products appear to be di- and mono-Me_2O-coordinated $[P_2Pt]^{2+}$ complexes (two OMe_2 peaks by ^1H NMR). A second asymmetric species, the $Pt_2(\mu$-BINOL) dimer **A**, was also observed; it forms whenever less than 2 equiv of acid (HOTf or $HBF_4{\cdot}O(CH_3)_2$) is added to **1a**. See ref 16 and a manuscript in progress for details.

(27) Note that when *rac*-**5** (90% endo) was used for the dppe experiment, an additional species (1:1 ratio compared to the original major species) whose ^{31}P NMR spectrum was almost coincident with that of **8a** was observed, even though the dppe ligand is achiral. Two sets of resonances due to Pt-coordinated **5** were seen by ^1H NMR. At present, these data cannot be satisfactorily explained.

Table 2. Equilibrium Constants for Relative Ligand Coordination to $[P_2Pt]^{2+}$

Entry	Equilibrium	K_{eq}^{dppe}	$K_{eq}^{R\text{-}BINAP}$
1	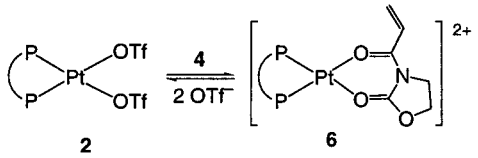	60(20)[a]	90(50)[a]
2	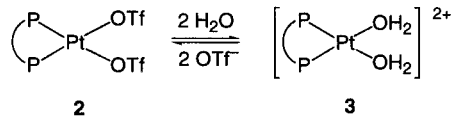	>14,000[b]	>14,000[b]
3	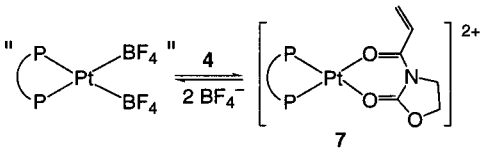	>1100[b]	>1100[b]
4	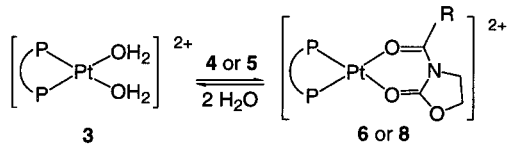	<0.01[b]	<0.01[b]
5	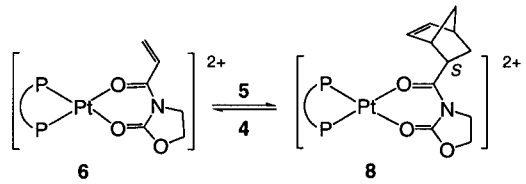	20(10)[c]	2.5[c,d]

[a] Average over 5−7 experiments with 1.5−10 equiv of **4**. [b] Calculated assuming a detection limit of 1% for minor species by ^{31}P NMR. [c] All major and minor resonances of **8** were included in the calculation of K_{eq}, while residual **2** (<3%) was not. Experiments with *rac*- and 2*S*-**5** gave the same K_{eq} value. [d] Two experiments gave the same K_{eq} value.

amount of **6b** present. Ambiguous results were also observed when **3b** was treated with *rac*-**5**; no **8b** was formed, but unidentified resonances appeared upfield of **3b** and grew disproportionately large when more *rac*-**5** was added to the solution.

To directly compare the abilities of dienophile **4** (reaction substrate) and Diels−Alder adduct **5** (reaction product) to bind to the Pt Lewis acids, **2** was generated in the presence of both 10 equiv of **4** and 1.5−2 equiv of 2*S*-**5**. Figure 2 shows the ^{31}P NMR spectrum afforded by the dppe version of this experiment; K_{eq} for the **6**/**8** (**4**/**5**) equilibrium in entry 5 of Table 2 was calculated from the spectral integration data. K_{eq} for the *R*-BINAP case was measured similarly.

Finally, the dppe and *R*-BINAP Lewis acids $P_2Pt(OTf)_2$ (**2a** and **2b**, respectively) were allowed to compete directly for binding to dienophile or Diels−Alder adduct. When 2 equiv each of Lewis acids **2a** and **2b** was generated in the presence of 1 equiv of **4**, no free **4** was observed by ^1H NMR, while **2a**, **2b**, **6a**, and **6b** were visible in the ^{31}P NMR spectrum of the equilibrium reaction mixture (Figure 3), affording the K_{eq} value in entry 1 of Table 3. An analogous competition experiment conducted with 2*S*-**5** instead of **4** gave K_{eq} for entry 2. To better contrast the relative **4**/**5** binding preferences of the two $[P_2Pt]^{2+}$ Lewis acids, the equilibrium in entry 3 (Table 3) was *calculated* in two ways: (1) by addition of the reverse of entry 1 to entry 2 or (2) by addition of the reverse of the *R*-BINAP **6**/**8** equilibrium in entry 5 of Table 2 to the dppe **6**/**8** equilibrium in entry 5 of Table 2. Two K_{eq} values for the new equilibrium were calculated from the two sets of data, providing a convenient check of the internal consistency of the thermodynamic data in Tables 2 and 3.

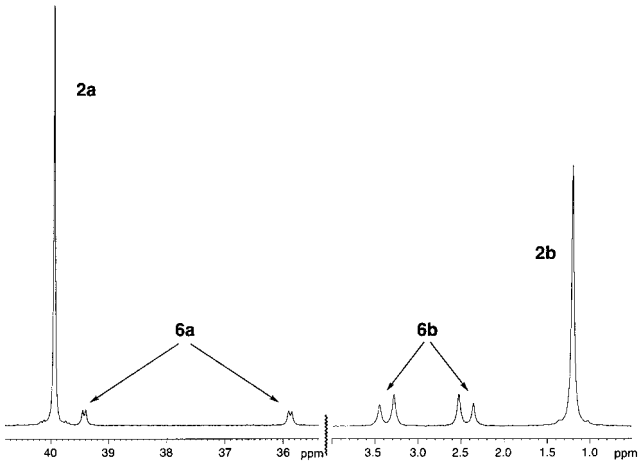

Figure 3. ^{31}P NMR spectrum (400 MHz) of an experiment in which **2a** and **2b** competed for coordination to **4**, yielding an equilibrium mixture of **2a**, **2b**, **6a**, and **6b** (entry 1, Table 3). Platinum satellites are not shown.

Table 3. Equilibrium Constants for 2a/2b Competition Experiments

Entry	Equilibrium	K_{eq}
1	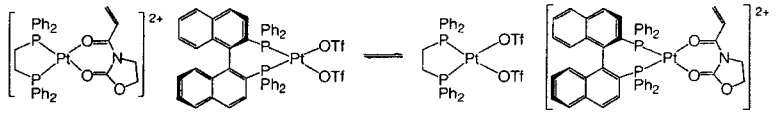	2.8[a]
2	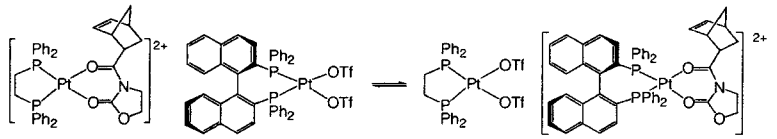	1.6[a]
3	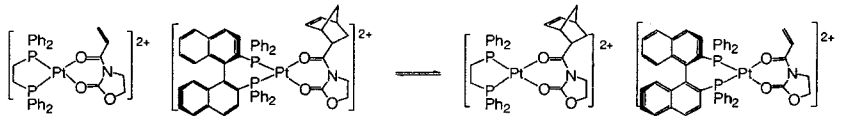	2[b] or 9[c]

[a] Single experiment. [b] Calculated from entries 1 and 2, Table 3: 2.8/1.6 = 1.8. [c] Calculated from entry 5, Table 2: 20/2.5 = 9.2.

Scheme 5

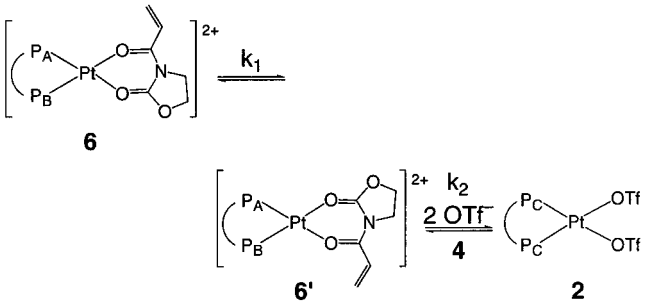

(4) Measurement of Ligand Exchange Rates via Dynamic ^{31}P NMR. The rates of dienophile/dienophile and OTf^-/dienophile exchange were examined as a function of temperature via line shape analysis of broadened ^{31}P NMR spectra of a **2**/**6** equilibrium mixture (Table 2, entry 1). The spectra were acquired at temperatures between 190 and 320 K and were simulated using the program DNMR3 in conjunction with SpinWorks, yielding the rates (k, s^{-1}) of ligand exchange at each temperature.[28] Since two different exchange processes were apparent from the ^{31}P spectra, two different rates (k_1 and k_2) were varied to fit the experimental data. In the first type of exchange (k_1), which occurred at lower temperatures, the two doublets of Pt–oxazolidinone complex **6** broadened and eventually coalesced into a single resonance, indicating mutual exchange of the nonequivalent phosphorus nuclei P_A and P_B in **6** (Scheme 5). The second type of exchange (k_2) was marked by broadening and coalescence of the resonances for **2** and **6**, indicating that OTf^-/**4** ligand substitution occurs (Scheme 5). Although k_1 and k_2 were determined over a range of temperatures in both the dppe and *R*-BINAP systems, 270 K was the only temperature at which well-defined values for both k_1 and k_2 could be obtained for both the *R*-BINAP and dppe complexes. Therefore, exchange rates for the P_2Pt^{II} complexes are reported and compared at this temperature (Table 4).[29]

Table 4. Ligand Exchange Rates[a] for P_2Pt^{II} Complexes in CD_2Cl_2 at 270 K

	dppe	R-BINAP
k_1	8400(300)	47(1)
k_2	26(1)	2(0.2)

[a] Uncertainties in k_1 and k_2, given in parentheses, were estimated by noting the range of values that produced visually indistinguishable simulated ^{31}P NMR spectra.

Attempts to measure the rates of other ligand exchange processes using line shape analysis were not successful. For example, broadened spectra of a **2**/**6**/**8** equilibrium mixture (Table 2, entry 5) proved impossible to simulate because too many types of exchange (dienophile/dienophile, cycloadduct/cycloadduct, dienophile/cycloadduct, OTf^-/dienophile, and OTf^-/cycloadduct) were occurring at once, while BF_4^-/dienophile and H_2O/dienophile exchange rates were inaccessible because the equilibrium strongly favored one of the complexes (Table 2, entries 3 and 4).

Discussion

(1) In Situ Characterization of Lewis Acid–Lewis Base Complexes. A prerequisite to examination of the mechanism of any transition-metal-catalyzed organic transformation is the ability to observe, in situ, the organometallic species present during the reaction. As pointed out in the Introduction, a combination of fortuitous properties make the P_2Pt^{II} Lewis acid–Lewis base complexes formed during the $P_2Pt(OTf)_2$-catalyzed Diels–Alder reaction (eq 1) amenable to characterization by ^{31}P and ^1H NMR spectroscopy at 195 K. Using NMR methods, the active catalysts **2**, as well as catalyst–substrate complexes **6**, catalyst–product complexes **8**, and even complexes (**3**) of the Pt Lewis acids

(28) SpinWorks Version 1.2 is copyright 1999–2001 by Kirk Marat, The University of Manitoba, Winnipeg, Manitoba, Canada R3T 2N2. The original authors of DNMR3 were G. Binsch and D. Kleier of the University of Notre Dame, South Bend, IN 46556.

(29) See the Supporting Information for plots of ln k_1 and ln k_2 vs $1/T$ (K) for the dppe and *R*-BINAP complexes.

with water (a common impurity or additive in these reactions) could be observed as stable, nonfluxional species in CD_2Cl_2 solution at low temperature. ^{31}P NMR spectra were particularly informative, as they indicated that both dienophile **4** and Diels−Alder adduct **5** coordinate to $[P_2Pt]^{2+}$ in a bidentate fashion via their carbonyl group oxygens, producing nonsymmetric chelate complexes (**6** and **8**) with large P−Pt coupling constants, consistent with formation of weak Pt−O=C bonds (Scheme 3, Table 1). Observation of this "traditional" coordination mode for **4** and **5** strongly suggests that the $P_2Pt(OTf)_2$ Lewis acids do catalyze the Diels−Alder reaction by a typical Lewis acid mechanism (Scheme 1). Thus assured that complexes **2**, **6**, and **8** (and sometimes **3**) are stable and present in solution during **2**-catalyzed Diels−Alder reactions, the thermodynamic (section 2 below) and kinetic relationships (section 3 below) between these complexes were investigated to further illuminate the details of the catalytic reaction mechanism.

(2) Thermodynamic Relationships: Competitive Binding of Lewis Bases to $[P_2Pt]^{2+}$. Dienophile (4) vs Counterion (OTf^- or BF_4^-). The ability of a Lewis acid to coordinate and activate Lewis basic substrates is fundamentally important to successful Lewis acid catalysis. The favorable triflate/dienophile equilibrium constant (Table 2, entry 1) observed when **4** was added to $P_2Pt(OTf)_2$ (**2**) demonstrates a thermodynamic bias for formation of the complex (**6**) necessary for dienophile activation. Although triflate is generally considered to be the "most coordinating" of the weakly coordinating counterions, coordination of OTf^- to Pt evidently does not significantly inhibit dienophile binding to the Lewis acid. Nevertheless, experiments performed by Ghosh and in our own laboratory have shown that "$P_2Pt(BF_4)_2$" Lewis acids are more active than OTf^- catalysts for the Diels−Alder reaction in eq 1;[6a,30] therefore, the effect of the counterion on dienophile binding to $[P_2Pt]^{2+}$ was also examined (Table 2, entry 3). As expected, displacement of BF_4^- by **4** is more thermodynamically favorable than displacement of OTf^- (K_{eq} >1100 for BF_4^- vs 60−90 for OTf^-), consistent with the conventional wisdom that BF_4^- is "less coordinating" than OTf^-.

Comparison of K_{eq} values for the dppe and *R*-BINAP equilibria in entry 1 of Table 2 reveals that K_{eq} is only slightly larger in the *R*-BINAP case than in the dppe case (90 vs 60), despite significant steric and electronic differences between the two diphosphines. The larger, less basic, triaryl-substituted phosphine *R*-BINAP should generate an $[(R\text{-BINAP})Pt]^{2+}$ fragment that is bulkier but significantly more electrophilic than the $[(dppe)Pt]^{2+}$ Lewis acid. These properties could cause steric inhibition of ligand binding and associative ligand exchange processes in the *R*-BINAP Lewis acid or they might cause it to bind Lewis bases more strongly (potentially activating coordinated dienophiles more strongly to attack by dienes). Nevertheless, these differences are not manifested in the similar binding preferences of the dppe and *R*-BINAP $[P_2Pt]^{2+}$ catalysts for **4** over OTf^-.

Water vs Dienophile (4) or Diels−Alder Adduct (5). Competitive coordination of Lewis bases other than the substrate to the catalyst may also affect the efficiency of Lewis acid catalyzed reactions. For example, additives such as water, alcohols, and amines have been shown to affect the turnover rates of some Lewis acid catalyzed reactions.[31] With the *R*-BINAP Lewis acid **2b**, Ghosh observed significant acceleration of Pt-catalyzed Diels−Alder reactions when 2 equiv of water was added to the catalyst (from 20 to 1 h for 100% conversion, 20 mol % catalyst).[6a] However, the experiments described here clearly show that water binds more strongly to $[P_2Pt]^{2+}$ than any of the other Lewis bases examined. This conclusion is supported by the following facts. (1) The P−Pt coupling constants of diaqua complexes **3** are smaller than those of any other P_2Pt^{II} species, indicating that water exerts the strongest trans influence on phosphorus of any of the oxygen-based ligands studied herein (Table 1).[21] (2) Two equivalents of water displaced OTf^- from $P_2Pt(OTf)_2$ quantitatively (Table 2, entry 2), demonstrating that water binds much more strongly to Pt than triflate. (3) Neither dienophile **4** nor cycloadduct **5** was able to substantially displace Pt-coordinated water from **3** (Table 2, entry 4), although the observation of species other than **3b** in the *R*-BINAP experiments may indicate that displacement of water by **4** or **5** is more thermodynamically favorable in this system than in the dppe case. Thus, we predicted (and observed),[32] on the basis of thermodynamic considerations, that water should act as a competitive inhibitor during Diels−Alder catalysis, rather than accelerating catalysis as observed by Ghosh.

Dienophile (4) vs Diels−Alder Adduct (5). During Lewis acid catalyzed reactions, competitive coordination of reaction product to the catalyst (product inhibition) may significantly inhibit catalytic turnover, making high catalyst loading necessary to achieve satisfactory conversion. To assess the potential for product inhibition in $P_2Pt(OTf)_2$-catalyzed Diels−Alder reactions, competition experiments were conducted to see whether substrate **4** or product **5** binds more strongly to $[P_2Pt]^{2+}$. These reactions showed that both the dppe and *R*-BINAP Lewis acids exhibit small thermodynamic preferences for coordination to 2*S*-**5** rather than **4** (Table 2, entry 5). The fact that $[(dppe)Pt]^{2+}$ prefers 2*S*-**5** over **4** more strongly than does $[(R\text{-BINAP})Pt]^{2+}$ (K_{eq} = 20 vs 2.5) suggests that steric factors may be more important in determining the relative binding of Lewis bases to **2b** than they are in the case of **2a**. For example, catalyst−product complex *R*,2*S*-**8b** may be destabilized relative to catalyst−dienophile complex **6b** in the *R*-BINAP system due to steric interactions of the bulky *R*-BINAP ligand with 2*S*-**5**, which are not as severe with

(30) (a) Becker, J. J.; Gagné, M. R. Unpublished results. (b) Evans, D. A.; Murray, J. A.; Matt, P. V.; Norcross, R. D.; Miller, S. J. *Angew. Chem., Int. Ed. Engl.* **1995**, *34*, 798−800.

(31) (a) Koh, J. H.; Larsen, A. O.; Gagné, M. R. *Org. Lett.* **2001**, *3*, 1233−1236. (b) Vogl, E. M.; Gröger, H.; Shibasaki, M. *Angew. Chem., Int. Ed. Engl.* **1999**, *38*, 1570−1577.

(32) In fact, our own Diels−Alder catalysis studies, conducted as reported in the following paper using catalysts prepared in situ from **1**, are consistent with water acting as a poison in the present system, in contrast to Ghosh's results. For example, at −40 °C the addition of 1, 2, and 4 equiv of H_2O to $(R\text{-BINAP})Pt(OTf)_2$ led to decreases in product conversion (eq 1, 140 min) from 99% to 96, 73, and 47%, respectively (however, the ee was 96−98% in all cases). Although we have no satisfactory explanation for the discrepancy between these observations and Ghosh's, we note that reactivity differences do occur, depending on how the $[P_2Pt]^{2+}$ catalyst was generated (e.g. P_2PtCl_2 + AgOTf vs $P_2Pt(BINOL)$ + HOTf). Apparently the Ghosh methodology of protonating the salicylate accesses a highly selective, albeit uncharacterized, catalyst that is subject to strong rate accelerations in the presence of water.

the smaller, flatter ligand **4**. These steric differences likely matter less in the less bulky dppe system, making **6a** and **8a** closer in energy than **6b** and *R*,2*S*-**8b**. Superimposed on the steric differences between dienophile and product are their electronic differences. Treating the imide as an ester leads to the prediction that 2*S*-**5** should be more basic than dienophile **4**, since the carbonyl group of an α,β-unsaturated ester is less basic than that of the saturated analogue (although the opposite is true for aldehydes and ketones).[33] Thus, we infer that the binding constant for P_2 = dppe more closely reflects the inherent basicity of the competing ligands, while the binding constant for P_2 = *R*-BINAP is attenuated by the opposing effects of basicity and the increased congestion of the product/BINAP complex. Moreover, the difference in the dppe and *R*-BINAP K_{eq} values also indicates that product inhibition should be more severe in **2a**-catalyzed than in **2b**-catalyzed Diels–Alder reactions.

A more direct way to compare the **4**/2*S*-**5** binding preferences of the dppe and *R*-BINAP Lewis acids, particularly with respect to the potential for product inhibition, was provided by experiments in which **2a** and **2b** competed for binding to **4** or to 2*S*-**5** (Table 3, entries 1–2). The small K_{eq} value of 2.8 for the equilibrium in entry 1 reflects a slight thermodynamic preference of *R*-BINAP Lewis acid **2b**, relative to dppe Lewis acid **2a**, for binding **4** over OTf^-. The smaller K_{eq} value (1.6) for entry 2 shows that both catalysts bind **5** over OTf^-, with similarly favorable thermodynamics. Taken together, these results again indicate that the ground-state energy difference between dppe complexes **6a** and **8a** is greater than the corresponding difference between *R*-BINAP complexes **6b** and *R*,2*S*-**8b** ($K_{eq} > 1$ in entry 3, Table 3); therefore, product inhibition should be greater in **2a**-catalyzed Diels–Alder reactions. As a check of the internal consistency of the K_{eq} data, K_{eq} for the equilibrium in entry 3 was also calculated from the equilibrium constants for the dppe and *R*-BINAP **4**/**5** equilibria in entry 5 of Table 2. Within experimental error, this K_{eq} value matched that calculated from entries 1 and 2 of Table 3 (1.8 ± 1.2 vs 9.2 ± 6.1).

Summary of the Relative Binding Strengths of Lewis Bases to $[P_2Pt]^{2+}$. A scale of relative binding strengths for the catalytically important Lewis bases **4**, **5**, H_2O, OTf^-, and BF_4^- to Diels–Alder catalysts $[P_2Pt]^{2+}$ at 195 K was assembled from the thermodynamic data described above. For dppe, the scale is $BF_4^- \ll OTf^- < \mathbf{4} < \mathbf{5} \ll H_2O$, which also correlates with the P–Pt coupling constants observed for complexes of the Lewis bases with $[P_2Pt]^{2+}$: $^1J_{P-Pt}$ = 4170 (OTf (**2a**)) > 4080/4000 (**4** (**6a**)) ≥ 4200/3950 (**5** (**8a**)) > 3950 (H_2O (**3a**)) (Table 1; see also Scheme 7, vide infra). As expected, the weakest ligands exert the weakest trans influence on the diphosphine ligand.[21] A similar binding scale constructed for the *R*-BINAP Lewis acid includes the differential binding of cycloadduct enantiomers 2*S*- and 2*R*-**5**: $BF_4^- \ll OTf^- < \mathbf{4} <$ 2*R*-**5** < 2*S*-**5** $\ll H_2O$. Although the major cycloadduct enantiomer produced by [(*R*-BINAP)Pt]$^{2+}$ Lewis acid catalysis, 2*S*-**5**, does coordinate more strongly to the Lewis acid than the minor enantiomer 2*R*-**5** (65:35 thermodynamic preference, $\Delta G_{2S,2R}$ = 0.24 kcal mol^{-1} at −78 °C), note that

(33) For instructive references, see ref 15a,b.

Scheme 6

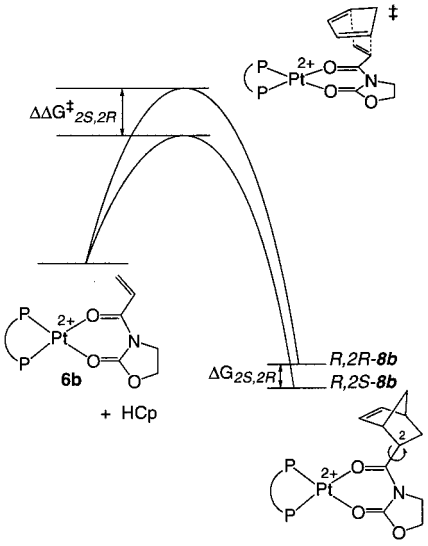

the competing diastereomeric Diels–Alder transition states must be significantly more different in energy (k_{2S}/k_{2R} = 98/2, $\Delta\Delta G^{\ddagger}_{2S,2R}$ = 1.7 kcal mol^{-1} at −50 °C) to produce 2*S*-**5** in the observed 96% ee (Scheme 6). This difference between the diastereomeric ground and transition states is likely due to stereoelectronically imposed orbital overlap between the incoming diene and the activating carbonyl group of the Pt-coordinated dienophile in the transition state, an interaction which rigidifies this structure and creates a conformational restriction not present in **8b**. The additional rotational degree of freedom in the coordinated product relaxes the diastereomer-discriminating steric interactions between *R*-BINAP and 2*S*- or 2*R*-**5** and levels the ground-state energies of *R*,2*S*- and *R*,2*R*-**8b** (Scheme 6).

(3) Kinetic Relationships: Ligand Exchange in Lewis Acid–Lewis Base Complexes. Since ligand substitution reactions are essential to achieve both substrate activation and product release (turnover) in a catalytic cycle, the rates of ligand exchange for the $[P_2Pt]^{2+}$ Lewis acid–Lewis base complexes were investigated by dynamic ^{31}P NMR spectroscopy. Simulation of exchange-broadened spectra of a $P_2Pt(OTf)_2$/$[P_2Pt(\mathbf{4})]^{2+}$ (**2**/**6**) equilibrium mixture (entry 1, Table 2) afforded the rates of two different exchange processes (k_1 and k_2) at 270 K for both the dppe and *R*-BINAP complexes (Table 4). As described in Results, the first exchange process (rate = k_1) equilibrates the nonequivalent phosphorus nuclei P_A and P_B of Pt–oxazolidinone complex **6**, while the second type of exchange (rate = k_2) corresponds to OTf^-/dienophile ligand substitution (Scheme 5). Possible mechanisms for the former exchange process include attack of either OTf^- or a second molecule of **4** on the Pt center of **6**, followed by pseudorotation of the five-coordinate intermediate and release of the nucleophile.[34] Such a dynamic process does not result in net displacement of the dienophile from the catalyst (i.e., does not affect turnover during catalysis). This exchange occurs more quickly than the OTf^-/**4** exchange process measured by k_2 in both the

(34) The putative 5-coordinate intermediate obtained from OTf^- addition to **6** is also a reasonable intermediate in the OTf^-/**4** exchange process.

Scheme 7

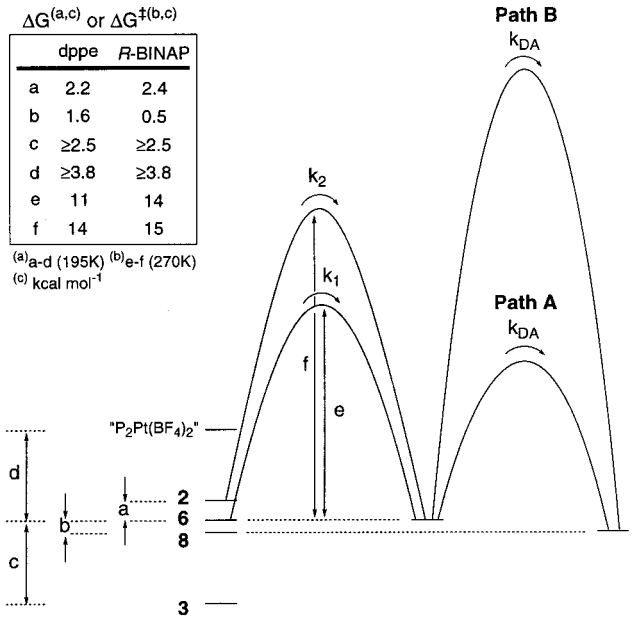

dppe and *R*-BINAP cases ($k_1/k_2 = 320$ for dppe; 24 for *R*-BINAP). More importantly, however, a significant difference in the ligand exchange rates of dppe and *R*-BINAP Pt complexes was observed: k_1 was 180 times faster for dppe than for *R*-BINAP complexes, while k_2 was 13 times faster for dppe. These diphosphine-dependent rates may differ due to disparities in the steric bulk of the two phosphines (the bulky *R*-BINAP ligand may inhibit associative ligand attack on the Pt center), disparities in ligand electronics (the more electrophilic (*R*-BINAP)Pt center may bind more strongly to Lewis bases, making ligand displacement less facile), or a combination of both these factors.

(4) Kinetics, Thermodynamics, and Pt Diels–Alder Catalysis. The thermodynamic and kinetic relationships between complexes of the Lewis bases OTf^-, BF_4^-, **4**, **5**, and H_2O with the $[P_2Pt]^{2+}$ Lewis acids are summarized in the left half of the simplified free energy diagram in Scheme 7. (Free energy values ΔG and $\Delta G^‡$ were calculated from the K_{eq} and rate data, at 195 and 270 K, respectively.) This picture contrasts the small ground-state energy differences between the P_2Pt^{II} complexes ($\Delta G = 0.5–4$ kcal mol^{-1}) with the much larger energy barriers observed for interconversion of the complexes via ligand substitution reactions ($\Delta G^‡ = 11–15$ kcal mol^{-1}); the latter values are also more variable than the former, depending on both the mechanism for ligand substitution (k_1 vs k_2) and the identity of the diphosphine (dppe vs *R*-BINAP).

The right half of the diagram depicts two possible free-energy barriers to the interconversion of **6** and **8** via a Pt-catalyzed cycloaddition reaction (Scheme 7). If the barrier to cycloaddition is lower than the barriers observed for ligand exchange (path A), then HCp attack on Pt-bound **4** will occur at a faster rate than ligand exchange ($k_{DA} > k_1$ and k_2), making ligand exchange the turnover-limiting step of the catalytic cycle (Scheme 1). On the other hand, a cycloaddition barrier higher than the barriers to ligand substitution (path B) indicates that the cycloaddition step itself is the slow, turnover-limiting step of the catalytic cycle (Scheme 1). To investigate which scenario applies to the **2**-catalyzed Diels–Alder reactions in question, 5 equiv of HCp was added to Pt–dienophile complexes **6** at 195 K, and the reaction to give **8** was monitored by ^{31}P and ^1H NMR at this temperature. These NMR spectra showed that all of the Pt-coordinated **4** present was immediately converted to Pt-coordinated **5** on addition of diene; no trace of **6** was visible by NMR at any time after HCp addition in both the dppe and *R*-BINAP systems.[35] Most important, no turnover was observed in the *R*-BINAP reaction at this temperature, confirming that cycloaddition (k_{DA}) is faster than ligand exchange (k_1 and k_2), making the latter the turnover-limiting step of the catalytic cycle (path A, Scheme 6). Consistent with this interpretation, the turnover frequency of **2b**-catalyzed Diels–Alder reactions (reported in the following paper) are smaller than and within an order of magnitude of the OTf^-/**4** exchange rates k_2 determined here (Table 4).[16]

Because ligand exchange rather than cycloaddition is the turnover-limiting step of the $P_2Pt(OTf)_2$-catalyzed Diels–Alder reaction, the organometallic species present in the reaction solution (**2**, **6**, and **8**) never reach thermodynamic equilibrium under catalysis conditions. Instead, **6** is quickly converted to **8** by the cycloaddition step as soon as it forms via the ligand substitution step; thus, only small, steady-state concentrations of **6** are expected to be present in solution; the catalyst resting state will be **8**. Under these conditions, the thermodynamic relationships between **2**, **6**, and **8** probably have little effect on the turnover rates of $P_2Pt(OTf)_2$-catalyzed Diels–Alder reactions.

Conclusions

Through in situ observation of $P_2Pt(OTf)_2$ catalysts **2**, catalyst–substrate complexes **6,** and catalyst–product complexes **8** using ^{31}P and ^1H NMR spectroscopy at 195 K, we have confirmed that **2**-catalyzed Diels–Alder reactions (eq 1) proceed by the expected Lewis acid activation of dienophile **4**, via coordination of its carbonyl groups to the Pt catalyst (Scheme 1). Investigation of the thermodynamic relationships between **2**, a BF_4^- analogue of **2**, and the Pt Lewis acid–Lewis base complexes **3**, **6**, and **8** led to the following conclusions. (1) Coordination of OTf^- to Pt does not thermodynamically impede binding of substrate **4** to the Lewis acid catalyst, although BF_4^- inhibits dienophile binding even less, consistent with its perception as a "less coordinating" counterion than OTf^-. (2) Water does competitively inhibit binding of **4** to the catalyst. (3) Product inhibition should be more significant in (dppe)$Pt(OTf)_2$-catalyzed than in (*R*-BINAP)$Pt(OTf)_2$-catalyzed Diels–Alder reactions. The thermodynamic relationships between the complexes studied were also summarized by a scale of the relative binding strengths of the Lewis bases to $[P_2Pt]^{2+}$ ($BF_4^- \ll OTf^- < \mathbf{4} < \mathbf{5} \ll H_2O$).

Investigation of the kinetic relationships between $P_2Pt(OTf)_2$ and $[P_2Pt(\mathbf{4})]^{2+}[OTf]^-_2$ via simulation of dynamic ^{31}P NMR spectra of a **2**/**6** equilibrium mixture revealed that two different exchange processes (**4**/**4′** and

(35) Additional mechanistic information was obtained by monitoring the Pt-catalyzed Diels–Alder reactions in situ by ^{31}P and ^1H NMR at 195 K. See ref 16.

OTf^-/**4**) occur and that the rates (s^{-1}) of both are 1–2 orders of magnitude faster for dppe than for *R*-BINAP complexes. Also, experiments in which the reaction of HCp with **6** was monitored by ^{31}P and ^1H NMR at 195 K enabled comparison of the rates of **6**/**8** interconversion via cycloaddition reactions with the rates of **6**/**8** interconversion via ligand exchange reactions. Observation of immediate and quantitative conversion of **6** to **8** upon addition of HCp, but *no catalytic turnover*, clearly demonstrated that cycloaddition is much faster than ligand substitution, making ligand exchange the turnover-limiting step of the catalytic cycle (Scheme 1).

From all the kinetic and thermodynamic data reported here, the rates of ligand substitution processes emerge as the most important factors controlling the activity of $P_2Pt(OTf)_2$ Lewis acids **2** as catalysts for the Diels–Alder reaction (eq 1). The fact that ligand exchange rather than cycloaddition kinetics determine the overall efficiency of $[P_2M]^{2+}$-catalyzed reactions leads to the obvious conclusion that the turnover rates of these processes may be increased by accelerating ligand substitution reactions, and *not* by further enhancing the metal center's electrophilicity. Indeed, our data indicate that despite being considered "soft", late-metal Lewis acids are extremely electrophilic, as judged by the fact that Pt-coordinated dienophiles undergo cycloaddition very rapidly at 195 K (clearly, **4** is strongly activated by coordination to Pt). This scenario, in which ligand substitution rates rather than electrophilicity dominate catalytic activity, suggests that $[P_2Pd]^{2+}$ Lewis acid catalysts are more active than their Pt analogues for transformations such as the Diels–Alder reaction because ligand substitution dynamics are faster, and not because the Pd centers are more electrophilic than Pt.

While perhaps counterintuitive in the context of typical substitution-labile Lewis acids, it is possible that when ligand exchange is turnover-limiting, decreasing the electrophilicity of the metal center might increase its catalytic activity by diminishing the strength of the exchanging Pt–ligand bonds enough to make ligand exchange more rapid. Such an enhanced ligand substitution rate may explain the observation that $P_2Pt(SbF_6)_2$ Lewis acids derived from **A** and $AgSbF_6$ (P_2 = *S*-2,2′-

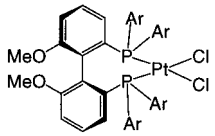

A

bis[(4-R-C_6H_4)phosphino]-6,6′-$(OMe)_2$-1,1′-biphenyl; R = ^{t}Bu, OMe, H, CF_3)[31a] are more active catalysts for glyoxylate-ene reactions when they contain electron-rich rather than electron-poor diphosphines, even though complexes derived from electron-poor ligands are presumably more electrophilic.

In conclusion, the combination of slow ligand substitution rates with excellent electrophilicity inherent in $[P_2M]^{2+}$ complexes suggests that these late-metal Lewis acid catalysts will continue to display reactivity and selectivity patterns that are distinct from those of early-metal, Cu(II)/Zn(II), and p-block Lewis acids.

Acknowledgment. We graciously thank the NIH (Grant No. GM60578), the Petroleum Research Fund, administered by the American Chemical Society, and Union Carbide for support of this research. We also thank the UNC Board of Governors and the ACS Division of Organic Chemistry for graduate Fellowships (N.M.B.). M.R.G. is a Camille-Dreyfus Teacher-Scholar (2000–2004).

Supporting Information Available: Text giving experimental details, plots of ln k_1 and ln k_2 vs $1/T$ (K) for **2a**/**6a** and **2b**/**6b** ligand exchange reactions, tables of atomic parameters, isotropic and anisotropic thermal parameters, bond distances, bond angles, and bond torsion angles for **2a**, and ^1H NMR spectra of **2a**, **2b**, **3a**, **3b**, **6a**, **6b**, **7a**, **7b**, **8a**, and *R*,2*S*-**8b**. This material is available free of charge via the Internet at http://pubs.acs.org.

OM0109861